Proc. Natl. Acad. Sci. USA
Vol. 89, pp. 7620–7624, August 1992
Medical Sciences

Regional mapping of prion proteins in brain

(β/A4-amyloid protein/brain mapping/Creutzfeldt–Jakob disease/histoblots)

ALBERT TARABOULOS*, KLAUS JENDROSKA†‡, DAN SERBAN*, SHU-LIAN YANG*, STEPHEN J. DEARMOND*‡, AND STANLEY B. PRUSINER*§¶

Departments of *Neurology, ‡Pathology, and §Biochemistry and Biophysics, University of California, San Francisco, CA 94143

Communicated by Theodore O. Diener, March 25, 1992 (received for review February 10, 1992)

ABSTRACT **Scrapie is characterized by the accumulation of a protease-resistant isoform of the prion protein PrP^{Sc}. Limited proteolysis and chaotropes were used to map the distribution of PrP^{Sc} in cryostat sections of scrapie-infected brain blotted onto nitrocellulose membranes, designated histoblots. Proteolysis was omitted in order to map the cellular isoform of the prion protein (PrP^{C}) in uninfected brains. Compared with immunohistochemistry, histoblots increased the sensitivity for PrP^{Sc} detection and showed different patterns of PrP^{Sc} accumulation. In Syrian hamsters with Sc237 scrapie, the most intense PrP^{Sc} signals occurred in sites with relatively little PrP^{C}, suggesting that aberrant localization of prion protein may be an important feature in the pathogenesis of prion diseases. Immunostaining of PrP^{Sc} in white-matter tracts suggested that prions spread along neuroanatomical pathways. PrP^{Sc} immunostaining in histoblots was quantitated by densitometry, permitting assessment of the extent of PrP^{Sc} accumulation within specific structures. Histoblots were also useful in localizing PrP^{CJD} and β/A4-amyloid peptide in the brains of patients with Creutzfeldt–Jakob disease and Alzheimer disease, respectively.**

Scrapie is the prototype of the transmissible neurodegenerative diseases caused by prions (1, 2), including Creutzfeldt–Jakob disease (CJD), Gerstmann–Sträussler syndrome (GSS), and kuru of humans as well as bovine spongiform encephalopathy (3). A host-encoded protein, the scrapie prion protein (PrP^{Sc}) (4–6), has been implicated as a necessary component of the prion (1, 7–10) as well as in the pathogenesis of scrapie (11, 12).

Because of the lack of scrapie-specific prion protein (PrP) antibodies (13) and the weak immunoreactivity of native PrP^{Sc} (14–18), the differential localization of the PrP isoforms in the scrapie brain could not be achieved with certainty by using traditional immunohistochemical methods. In particular, although PrP^{Sc}-containing extracellular amyloid plaques were easily distinguished (19), intracellular PrP^{Sc} immunostaining could not be unequivocally discriminated from the normal isoform PrP^{C} (14). Specific detection of PrP^{Sc} was achieved by limited proteolysis under conditions that hydrolyzed PrP^{C} followed by incubation with guanidine thiocyanate (GdnSCN) (17, 18). Because this approach could not be readily adapted to standard histological sections on glass slides, cryostat sections of unfixed brains were transferred to nitrocellulose membranes and lysed *in situ*. To detect PrP^{Sc} the membranes were then subjected to extensive proteolysis and treated with GdnSCN before immunostaining. The tissue sections processed by this method are called "histoblots." We used histoblots to map the distribution of PrP^{Sc} in the brains of Syrian hamsters inoculated with the prions and to determine the distribution of the normal isoform, PrP^{C}, in uninfected brains. Several variants of tissue printing and electroblotting have been reported (20–22).

The publication costs of this article were defrayed in part by page charge payment. This article must therefore be hereby marked "*advertisement*" in accordance with 18 U.S.C. §1734 solely to indicate this fact.

MATERIALS AND METHODS

Antibodies. Rabbit antisera RØ73 and RØ13 were raised against hamster PrP-(27–30) (17) and synthetic peptide PrP-P1 (23), respectively. The Syrian hamster PrP monoclonal antibody (mAb) 3F4 (15) was from R. Kascsak (Institute for Brain Research, Staten Island, NY). Its epitope, Met-Lys-His-Met, has been recently characterized (24, 25). 13A5 is a mAb obtained against hamster PrP-(27–30) (26). The following dilutions were used: antiserum RØ73, 1:5000; antiserum RØ13, 1:1000; mAb 13A5 supernatant, 1:2; mAb 3F4 ascitic fluid, 1:1000; and mAb 3F4 supernatant, 1:1. For absorption with synthetic peptides (Fig. 1), RØ13 antiserum or 3F4 ascitic fluid was diluted to 1:100 in 0.05% Tween 20/100 mM NaCl/10 mM Tris·HCl, pH 7.8 (TBST) and incubated for 1 hr with their respective free oligopeptides (250 μg/ml) before their use. Antiserum RØ13 was incubated with peptide PrP-P1 (23). mAb 3F4 was incubated with Pro_{102}-Ser-Lys-Pro-Lys-Thr-Asn-Met-Lys-His-Met. Rabbit antiserum R8271 was raised against a synthetic peptide corresponding to the 28 carboxy-terminal residues of the human β/A4-amyloid protein (17). The antiserum was used at a 1:1000 dilution.

Human Brain Specimens. The CJD brain was obtained from a 56-yr-old female in whom cerebrocortical biopsy showed spongiform degeneration and protease-resistant PrP (17). There was a 48-hr delay between death and freezing of the coronal brain sections. Studies on β/A4-amyloid deposition were done on a case of familial Alzheimer disease (AD) in a 40-yr-old male. The nonneurological case was a 61-yr-old male who died from cardiac insufficiency.

Inoculation of Hamsters and Mice. LVG:Lak random-bred Syrian hamsters and transgenic (Tg) mice expressing Syrian hamster PrP (7) were inoculated with 50 or 30 μl of brain extract into the thalamus, respectively (12, 28).

Histoblots. A nitrocellulose membrane was wetted in lysis buffer (0.5% Nonidet P-40/0.5% sodium deoxycholate/100 mM NaCl/10 mM EDTA/10 mM Tris·HCl, pH 7.8) and laid on a double layer of thick blotting paper saturated with lysis buffer. Glass slides carrying 8-μm-thick cryostat sections were quickly thawed, immediately pressed onto the membrane for 25 sec, and inspected for complete transfer of the section. Transfer was facilitated by a slow rotary motion that

Abbreviations: CJD, Creutzfeldt–Jakob disease; GSS, Gerstmann–Sträussler syndrome; AD, Alzheimer disease; PrP, prion protein; PrP^{Sc}, scrapie prion protein; PrP^{C}, cellular prion protein; Tg, transgenic; mAb, monoclonal antibody.

†Present address: Department of Neurology, Universitätsklinikum Rudolf Virchow, 1000 Berlin, Federal Republic of Germany.
¶To whom reprint requests should be addressed at: Department of Neurology, HSE-781, University of California, San Francisco, CA 94143-0518.

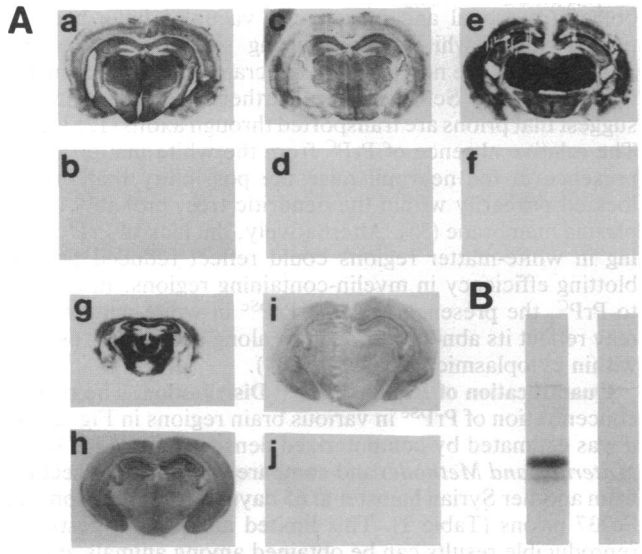

FIG. 1. Specific staining of PrP^{Sc} and PrP^{C} in histoblots of Syrian hamster brains. (*A*, *a–g*) PrP^{Sc} histoblots from a clinically ill Syrian hamster (*a*, *c–f*) and from a transgenic (Tg)(SHaPrP)81 mouse (*g*) after inoculation with Sc237 prions. Tg(SHaPrP)81 expresses the Syrian hamster PrP gene. The blots were probed with RØ73 (*a* and *b*), RØ13 (*c* and *d*), 3F4 (*e* and *f*), and 13A5 (*g*). No PrP^{Sc} was detected in uninfected, control Syrian hamster brain (*b*). Preincubation of RØ13 antiserum and mAb 3F4 with synthetic peptides carrying their respective epitopes abolished staining (*d* and *f*). (*h–j*) PrP^{C} histoblot of uninfected Syrian hamster immunoprobed with mAb 3F4 (*i* and *j*) or RØ73 antiserum (*h*). Preincubation of mAb 3F4 with the synthetic peptide carrying its epitope abolished staining (*j*). (*B*) Ten percent Syrian hamster brain homogenate was analyzed by SDS/PAGE (27), transferred to nitrocellulose, and probed with mAb 3F4. In the lane at right, preincubation of antibody with synthetic peptide abolished staining of PrP band.

prevented trapping of air bubbles. The membrane was left on the stack of blotting paper for several minutes.

For detection of PrP^{Sc} the membranes were thoroughly air dried, rehydrated for 1 hr in TBST and then subjected to limited proteolysis in digestion buffer (proteinase K at 400 μg/ml, for 18 hr at 37°C in 0.1% Brij 35/100 mM NaCl/10 mM Tris·HCl, pH 7.8) (17). The proteinase K concentration was reduced to 100 μg/ml for detection of PrP^{CJD} in the human case. To stop the reaction the blots were rinsed three times in TBST and incubated for 30 min in TBST/3 mM phenylmethylsulfonyl fluoride. Finally, the blots were incubated in 3 M GdnSCN/10 mM Tris·HCl, pH 7.8, for 10 min and rinsed three times in TBST before immunostaining. As a negative control we usually included the histoblot of a noninfected brain that did not contain PrP^{Sc} (Fig. 1*A*, *b*). PrP^{Sc} staining depended on the GdnSCN treatment, as expected from our prior experience with dot blots and immunofluorescence (17, 18) (data not shown).

To detect PrP^{C} in a normal brain, the blots were incubated for 1 hr in 100 mM NaOH and were then processed for immunostaining. This treatment considerably reduced background staining by solubilizing away the remnants of the tissue section from the membrane. The blots were then blocked with 5% nonfat dry milk/TBST and incubated for 18 hr at 4°C with the primary antibody in TBST/1% nonfat milk. The secondary antibody (alkaline phosphatase-conjugated) and its substrates were from Promega.

PrP Immunohistology on Cryostat Sections. Eight-micrometer sections of unfixed, snap-frozen brain were briefly dried, immersed for 5 min each in 50%, 100%, and 50% ethanol, and rehydrated in water before a 15-min incubation in 10% phosphate-buffered formalin. The tissue was then quenched for 5 min in 100 mM NH_4Cl and permeabilized by a brief immersion in 0.5% Nonidet P-40/phosphate-buffered saline; the proteins were then denatured by a 10-min incubation in 3 M GdnSCN/10 mM Tris·HCl, pH 7.8. After blocking with an overnight incubation in 10% goat serum/TBST/0.2% Tween 20, the sections were sequentially incubated with the PrP antiserum RØ73 (1:1000, 4 hr) and a biotinylated goat anti-rabbit IgG antibody (1 hr), both diluted in blocking buffer, and the antigen was detected with the ABC system (Vector Laboratories, Burlingame, CA).

PrP Densitometry on Histoblots. The regional relative concentration of PrP^{Sc} ([PrP^{Sc}]) was estimated by using a dissecting microscope with a charge-coupled device camera interfaced with a BQ system IV morphometric image analysis system (R & M Biometrics, Nashville, TN). A calibration curve relating average pixel density to [PrP^{Sc}] was generated by using proteinase K and GdnSCN-treated dot blots of brain lysates containing increased dilutions of PrP^{Sc} (17). To obtain dilutions of PrP^{Sc}, the lysate of a brain from a Syrian hamster with clinical signs of scrapie was serially diluted with a lysate of normal Syrian hamster brain. After immunostaining, an interactive curve was generated with the GRAPHPAD INPLOT curve-fitting program (San Diego, CA). Measurements of average pixel density in a brain region were made after defining the perimeter of the region followed by subtracting the mean background pixel density measured in three areas of the nitrocellulose paper surrounding the histoblot.

RESULTS

Detection of PrP^{Sc} and PrP^{C} on Histoblots. To ascertain the validity of the method, we immunostained histoblots of brain sections from a terminally ill Syrian hamster inoculated with Sc237 prions (29) (Fig. 1*A*, *a*, *c–f*) and from a terminally ill Tg(SHaPrP)81 mouse [expressing the Syrian hamster PrP gene (7)] with Sc237 scrapie (Fig. 1*A*, *g*). The histoblot from an uninfected hamster brain served as a negative control (Fig. 1*A*, *b*). Proteinase K− and GdnSCN-treated histoblots were stained with antiserum RØ73 (*a* and *b*), antiserum RØ13 (*c* and *d*), mAb 3F4 (*e* and *f*), and mAb 13A5 (*g*). All of these antibodies gave similar staining patterns in the sections of infected Syrian hamster brains (Fig. 1*A*, *a*, *c*, and *e*). The staining with antiserum RØ13 and mAb 3F4 was abolished by adsorption with synthetic peptides carrying their respective epitopes, demonstrating their specificity for PrP (Fig. 1*A*, *d* and *f*) (23–25). The histoblot from the uninfected brain remained unstained, confirming that the signal was confined to PrP^{Sc} and not to PrP^{C}. Finally, the hamster-specific mAb 13A5 detected PrP^{Sc} in the brain of the Tg(SHaPrP)81 mouse (*g*) but not in a blot from an infected non-Tg mouse that does not express Syrian hamster PrP (data not shown), demonstrating again the specificity of the signal.

PrP^{C} in the brains of uninfected animals was detected when proteolysis was omitted (Fig. 1*A*, *h–j*). mAb 3F4 (*i*) and antiserum RØ73 (*h*) yielded identical staining patterns, whereas preincubation of mAb 3F4 with a synthetic peptide carrying its epitope again completely abolished its staining (*j*).

Distribution of PrP Isoforms in Syrian hamster Brain. The pattern of PrP^{Sc} accumulation in Syrian hamster brains in the terminal stages of scrapie initiated by intrathalamic inoculation of Sc237 prions (Fig. 2, *c* and *d*) was compared with the distribution of PrP^{C} in uninfected brains (*e* and *f*) in coronal sections through the hippocampus–thalamus (Fig. 2, *c* and *e*) and through the septum–caudate nucleus (*d* and *f*). Two general features of the PrP distribution pattern were prominent: first, both PrP isoforms localized to specific anatomical structures, and second, in Syrian hamster brains inoculated with Sc237 prions, the most intense PrP^{Sc} signals occurred primarily in sites largely devoid of PrP^{C} in the uninfected, control Syrian hamster brains.

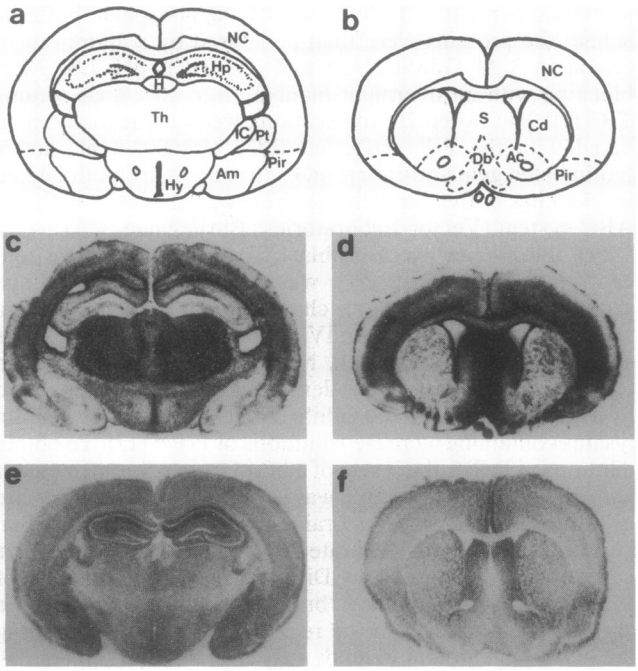

FIG. 2. Distribution of PrP^{Sc} and PrP^{C} in Syrian hamster brain. Coronal sections through hippocampus–thalamus (*c* and *e*) and septum–caudate nucleus (*d* and *f*) from a Syrian hamster clinically ill after inoculation with Sc237 prions (*c* and *d*) and an uninfected, control animal (*e* and *f*) were stained for PrP^{Sc} (*c* and *d*) or PrP^{C} (*e* and *f*) by using the histoblot method. Anatomical regions are detailed in *a* and *b*: Ac, nucleus accumbens; Am, amygdala; Cd, caudate nucleus; Db, diagonal band of Broca; H, habenula; Hp, hippocampus; Hy, hypothalamus; IC, internal capsule; NC, neocortex; Pir, piriform cortex; Pt, putamen; S, septal nuclei; Th, thalamus (stained with PrP antiserum RØ73).

In the gray matter, PrP^{C} immunostaining was most intense in the stratum radiatum and stratum oriens of the CA1 region of the hippocampus and was virtually absent from the granule cell layer of the dentate gyrus and the pyramidal cell layer throughout Ammon's horn (Fig. 2*e*). A complex shift in the pattern of PrP immunostaining occurred in the hippocampal formation during scrapie (Fig. 2). Other regions that did not appear to contain PrP^{C} were the medial habenular nucleus, the medial septal nuclei, and the diagonal band of Broca. In contrast, these regions were intensely immunostained for PrP^{Sc}. In the amygdala, the opposite relationship was found: PrP^{C} was present in normal animals but in hamsters with scrapie, PrP^{Sc} was absent. This inverse relationship between the amounts of PrP isoforms, coupled with the spatial and temporal relationship between PrP^{Sc} accumulation and neuropathology (12, 14), argues that the aberrant localization of PrP during scrapie may be an important feature in the pathogenesis of prion diseases.

Whether PrP^{C} and PrP^{Sc} are located in white matter could not be resolved in earlier immunohistochemical studies (compare Fig. 4*a* and *b* with 4*c*) (14). In the present study, PrP^{C} immunoreactivity was minimal in the white matter of normal, uninfected brains, whereas significant PrP^{Sc} was found in virtually all white-matter tracts of Syrian hamsters inoculated with Sc237 prions. Multifocal PrP^{Sc} immunostaining in the caudate nucleus (Fig. 2*d* and 4*a*) is due to the bundles of myelinated axons that cross through it. In contrast, those tracts were not immunoreactive in normal, uninfected animals (Fig. 2*f*). Other regions of white matter, such as the corpus callosum, the anterior commissure, and the optic nerves were also immunopositive for PrP^{Sc} but stained only weakly for PrP^{C} in normal brains. The presence of PrP^{Sc} in white matter of animals with scrapie is of interest because both intra-axonal and intramyelin vacuoles have been reported in the white matter during scrapie in mice (30), although they are not a feature of scrapie in Syrian hamsters inoculated with Sc237 prions. Furthermore, these findings suggest that prions are transported through axons (12, 31, 32). The relative absence of PrP^{C} from the white matter and its presence in the neuropil raise the possibility that PrP^{C} is located primarily within the dendritic tree, probably on the plasma membrane (33). Alternatively, the lack of PrP^{C} staining in white-matter regions could reflect reduced protein-blotting efficiency in myelin-containing regions. In contrast to PrP^{C}, the presence of some PrP^{Sc} in white-matter tracts may reflect its abnormal transport along axons (12), perhaps within cytoplasmic vesicles (18, 34).

Quantification of Regional PrP^{Sc} Distribution. The relative concentration of PrP^{Sc} in various brain regions in Fig. 2*c* and *d* was estimated by computerized densitometry (Fig. 3) (see *Materials and Methods*) and compared with similar sections from another Syrian hamster at 65 days after inoculation with Sc237 prions (Table 1). This limited analysis suggests that reproducible results can be obtained among animals at comparable stages of the disease. When these results were compared with the relative concentrations previously obtained by immunoanalysis of brain regions pooled from six to eight Syrian hamsters with clinical signs of scrapie at comparable stages of the disease (12, 14), one difference was found. The amount of PrP^{Sc} relative to the thalamus obtained from homogenates was from 40% to 80% less than that estimated by histoblots. Whether this discrepancy is related to the relatively poorly defined limits of dissected brain regions or to extrapolating regional concentrations from a single coronal section in a histoblot needs to be examined.

Histoblots Detect both Diffuse Accumulations of PrP^{Sc} and PrP Amyloid Plaques. To determine what portion of PrP^{Sc} staining in histoblots corresponds to amyloid plaques, we compared histoblots of cryostat sections (Fig. 4 *a* and *b*) with serial sections that were fixed in formalin and stained by peroxidase immunohistochemistry (Fig. 4*c*) (14). The layers of intense punctate immunostaining in the ventricular lining

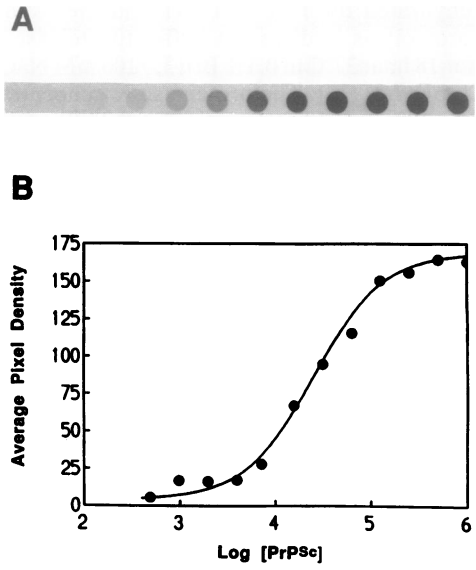

FIG. 3. Quantitation of PrP^{Sc} on nitrocellulose membranes by computerized densitometry. (*A*) Serial (half) dilutions of a scrapie Syrian hamster brain lysate were dotted on a nitrocellulose membrane. The lysate of an uninfected brain was used as diluent to keep the total amount of protein constant in all dots. The blot was treated with proteinase K and GdnSCN (17) and stained with rabbit antiserum RØ73. (*B*) The dot blot was then used to generate a calibration curve linking relative PrP^{Sc} content (in arbitrary units) of the dots to pixel density detected by the computerized densitometer.

Table 1. Regional levels in brains of scrapie-infected Syrian hamsters

Brain region	Relative levels of PrP^{Sc} in brain, arbitrary units	
	SHa A	SHa B
Thalamus	100*	100*
Hypothalamus	72	87
Hippocampus	59	22
Neocortex	47	49
Septum	193	182
Caudate nucleus	29	56

Two Syrian hamsters (SHa) designated A and B were sacrificed at 65 (A) and 70 (B) days after intracellular inoculation with $\approx 10^7$ ID_{50} units of Sc237 scrapie prions.
*Levels of PrP^{Sc} in various brain regions were determined by histoblotting relative to the thalamus, which was set at 100 arbitrary units.

(Fig. 4) and in the subcallosal region corresponded to PrP^{Sc} plaques seen in immunohistochemically stained tissue sections (Fig. 4*c*). In contrast, diffuse, nonamyloid PrP^{Sc} accumulation stained strongly in histoblots but very poorly in formalin-fixed, glass-mounted tissues (Fig. 4 *a* and *b*).

PrP^{CJD} in CJD and β-Peptide in AD. Humans with CJD and GSS accumulate protease-resistant PrP in the brain (35). In cases when no plaques are evident, the detection of PrP^{CJD} by standard immunohistology is difficult. Prompted by the histoblot results in the rodent system, we applied this methodology to the detection of PrP^{CJD} (Fig. 5*a*). A case of CJD was examined for the distribution of protease-resistant PrP by either histoblots (Fig. 5*a*) or a modified method termed "pressblot," in which the nitrocellulose paper was pressed to thawed slices of brain (data not shown). The blots were stained with mAb 3F4. Both methods yielded similar results; however, the staining pattern was more variable on pressblots, probably because of irregularities on the surface of brain slices (data not shown). Histoblots of two human CJD cases showed PrP^{CJD} confined to grey matter, which correlated with the distribution of spongiform degeneration and reactive gliosis (Fig. 5*a*). A nonneurological control brain prepared for histoblotting and immunostained at the same time did not contain detectable protease-resistant PrP (Fig. 5*b*).

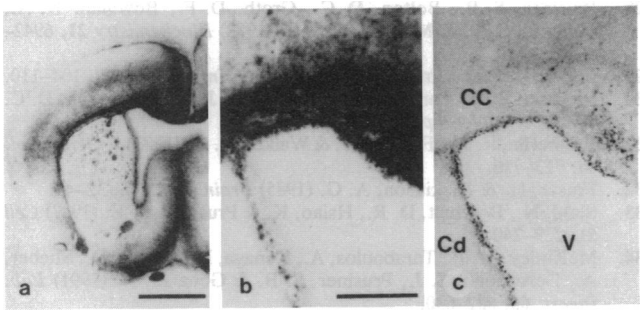

FIG. 4. PrP^{Sc} staining in histoblots and immunohistology. Serial coronal sections through the septum–caudate nucleus of Syrian hamster at 56 days after inoculation of Sc237 prions were either immunostained for PrP by using standard histological methods (*c*) or subjected to the histoblotting procedure before PrP^{Sc} staining (*a* and *b*). Comparison with the immunohistologic staining shows that punctated PrP^{Sc} accumulation in the lining of the ventricles (V) consists of plaques. More diffuse PrP^{Sc} depositions in the cortex and in the caudate nucleus (Cd), as well as strong PrP staining in the corpus callosum (CC) and in other white-matter regions, are not detectable by immunohistology. (Bars: *a*, 5 mm; *b* and *c*, 1 mm.)

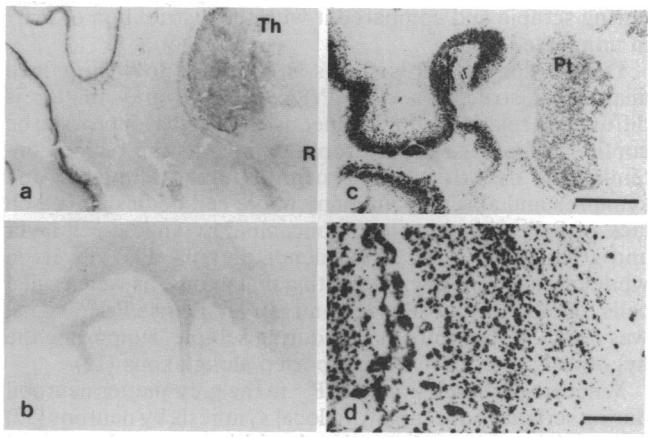

FIG. 5. Location of protease-resistant PrP^{CJD} in human CJD and protease-resistant β/A4 peptide in AD in histoblots/pressblots. (*a*) CJD histoblot of a coronal brain slice at level of thalamus (Th) and red nucleus (R) immunostained for PrP^{CJD} with mAb 3F4. An intense continuous band of immunostaining occurs throughout the cerebral cortex, primarily in its deeper layers, with weaker immunoreactivity occurring in more superficial layers. The thalamus, red nucleus, subthalamic nucleus adjacent to the latter, and remnants of the putamen between the thalamus and cortex are also immunopositive. (*b*) Histoblot of a nonneurological control brain that did not react with mAb 3F4. (*c*) AD pressblot from a coronal brain slice (thawed after storage at −70°C) from a case of familial AD immunostained by using the β/A4-peptide antiserum R8271. Punctate, plaque-like immunopositivity occurs in the cerebral cortex and the putamen (Pt). (*d*) Higher magnification of a histoblotted cryostat section from the frontal cortex of the same familial AD patient. At left is a β/A4-immunopositive blood vessel in the subarachnoid space (amyloid angiopathy). The full thickness of the cerebral cortex with numerous plaque-like β/A4 amyloid deposits extends to the right of the vessel. The subcortical white matter at far right contains scattered immunoreactive spots. CJD histoblots were treated with proteinase K at 100 μg/ml, whereas the standard 400 μg/ml concentration was used for AD histoblots. (Bars: *c*, 10 mm; *d*, 0.1 mm.)

It seemed likely that histoblots might also provide an efficient and sensitive method to map the distribution of β/A4-amyloid deposits in full-size coronal sections of human brain (17). We used the β/A4 antiserum R8271 to examine coronal sections by the pressblot (Fig. 5*c*) and the histoblot (Fig. 5*d*) methods. This case, along with three other cases of histologically confirmed nonfamilial AD (data not shown) produced similar plaque-like and vascular patterns of β/A4-amyloid immunostaining. Preincubation of the antiserum with the synthetic peptide reduced the staining intensity, confirming its specificity for β/A4-amyloid (data not shown).

The number of β/A4-amyloid immunoreactive spots outnumbered the number of senile plaques with amyloid cores identified in aldehyde-fixed sections stained with the same antibody or the Bielschowsky silver method (data not shown), suggesting that the method reveals β/A4-amyloid deposition in both classical and primitive amyloid plaques (36). In other regions of histoblots, diffuse β/A4-amyloid infiltration of the neocortex was found, which was similar to the pattern of PrP^{Sc} accumulation in the neocortex of humans and animals with prion diseases. Additionally, punctate β/A4 immunoreactivity was found in the white matter, similar to that previously described. No β/A4 amyloid deposits were found in the CJD case, and none of the four AD cases contained detectable PrP^{CJD} accumulation (data not shown).

DISCUSSION

The methods reported here allow specific immunodetection of both PrP isoforms in brain sections. We mapped the regional accumulation of PrP^{Sc} in brains of Syrian hamsters

during scrapie and compared it with the distribution of PrP^C in uninfected brains.

Distribution of PrP isoforms is restricted to well-defined anatomical structures. The PrP^C signal in grey matter is diffuse and relatively homogeneous. This signal appears to be confined largely to the neuropil, defined as the region containing the dendritic tree of neurons, axon terminals, and synapses and absent from many nerve cell bodies, based on lack of PrP^C signal in the hippocampal pyramidal-cell layer and granule-cell layer of the dendate gyrus. PrP^C levels in white matter were low, suggesting that axons, as well as glial cells, contain little PrP^C. In contrast, an intense PrP^{Sc} signal was found in the white matter during scrapie, supporting the hypothesis that PrP^{Sc} is transported along axons (12).

Whether accumulation of PrP^{Sc} in the grey-matter neuropil during scrapie is due largely to local synthesis by neurons (37) followed by transport to the dendritic tree or by axonal transport from distant neurons to a particular region is not known. Regardless of the mechanism leading to local deposition of PrP^{Sc}, its accumulation appears to underlie the development of clinically relevant neuropathology (12, 14).

By comparing histoblots with immunoperoxidase-stained serial frozen sections, we estimate that the method can resolve structures that are <25 μm apart. When histoblots are viewed with a dissecting microscope, subregional localization could be identified and correlated with specific neuronal groups. Individual PrP^{Sc} amyloid plaques, with diameters 10–25 μm were detectable in subependymal and subpial regions.

Histoblots were more sensitive than immunoanalysis of dissected brain regions for detection of PrP^{Sc}. For example, histoblots revealed focal PrP^{Sc} accumulation in the thalamus of Syrian hamsters $\approx$2 weeks before it was detected by immunoblot analysis (A.T. and S.J.D., unpublished observations). The intense histoblot signal revealed subregional accumulations of PrP^{Sc} in structures, such as the diagonal band of Broca, early in the course of scrapie in Syrian hamsters (38).

The amenability of the histoblot system to experimental manipulation and its high signal-to-noise ratio suggest that it may help in localizing molecules that are poorly detected by standard techniques, as in the case of fixation-sensitive antigens. The segregation of protease-resistant proteins from protease-sensitive isoforms can presumably be applied to other systems, especially to other amyloidoses.

Inclusion of detergent in the histoblot transfer buffer was probably responsible for the loss of structure at the cellular level (Fig. 4*b*). A recent study on the immunostaining of *fixed* tissue sections attached to membranes (39) raises the possibility that omission of the detergent will result in improved structure.

Histoblots have already proven useful in determining the distribution of PrP^{Sc} in the brains of hamsters and Tg mice inoculated with different isolates or "strains" of prions. Each isolate has been found to produce a specific pattern of PrP^{Sc} accumulation (38).

We thank Drs. F. Coufal, K. Hsiao, W. Mobley, and B. Oesch for helpful discussions and Mr. John McCulloch for photographic prints. This work was supported by research grants from the National Institutes of Health (AG02132, AG08967, NS14069, and NS22786), the American Health Assistance Foundation, as well as by gifts from Sherman Fairchild Foundation and National Medical Enterprises. K.J. was supported by a grant from the Deutsche Forschungsgemeinschaft (no. 145/5).

1. Prusiner, S. B. (1982) *Science* **216**, 136–144.
2. Prusiner, S. B. (1991) *Science* **252**, 1515–1522.
3. Wilesmith, J. W., Wells, G. A. H., Cranwell, M. P. & Ryan, J. B. M. (1988) *Vet. Rec.* **123**, 638–644.
4. Bolton, D. C., McKinley, M. P. & Prusiner, S. B. (1982) *Science* **218**, 1309–1311.
5. Chesebro, B., Race, R., Wehrly, K., Nishio, J., Bloom, M., Lechner, D., Bergstrom, S., Robbins, K., Mayer, L., Keith, J. M., Garon, C. & Haase, A. (1985) *Nature (London)* **315**, 331–333.
6. Oesch, B., Westaway, D., Wälchli, M., McKinley, M. P., Kent, S. B. H., Aebersold, R., Barry, R. A., Tempst, P., Teplow, D. B., Hood, L. E., Prusiner, S. B. & Weissmann, C. (1985) *Cell* **40**, 735–746.
7. Scott, M., Foster, D., Mirenda, C., Serban, D., Coufal, F., Wälchli, M., Torchia, M., Groth, D., Carlson, G., DeArmond, S. J., Westaway, D. & Prusiner, S. B. (1989) *Cell* **59**, 847–857.
8. McKinley, M. P., Bolton, D. C. & Prusiner, S. B. (1983) *Cell* **35**, 57–62.
9. Gabizon, R., McKinley, M. P., Groth, D. F. & Prusiner, S. B. (1988) *Proc. Natl. Acad. Sci. USA* **85**, 6617–6621.
10. Hsiao, K. K., Scott, M., Foster, D., Groth, D. F., DeArmond, S. J. & Prusiner, S. B. (1990) *Science* **250**, 1587–1590.
11. DeArmond, S. J., Kretzschmar, H. A., McKinley, M. P. & Prusiner, S. B. (1987) in *Prions—Novel Infectious Pathogens Causing Scrapie and Creutzfeldt–Jakob Disease*, eds. Prusiner, S. B. & McKinley, M. P. (Academic, Orlando, FL), pp. 387–414.
12. Jendroska, K., Heinzel, F. P., Torchia, M., Stowring, L., Kretzschmar, H. A., Kon, A., Stern, A., Prusiner, S. B. & DeArmond, S. J. (1991) *Neurology* **41**, 1482–1490.
13. Prusiner, S. B., Scott, M., Foster, D., Pan, K.-M., Groth, D., Mirenda, C., Torchia, M., Yang, S.-L., Serban, D., Carlson, G. A., Hoppe, P. C., Westaway, D. & DeArmond, S. J. (1990) *Cell* **63**, 673–686.
14. DeArmond, S. J., Mobley, W. C., DeMott, D. L., Barry, R. A., Beckstead, J. H. & Prusiner, S. B. (1987) *Neurology* **37**, 1271–1280.
15. Kascsak, R. J., Rubenstein, R., Merz, P. A., Tonna-DeMasi, M., Fersko, R., Carp, R. I., Wisniewski, H. M. & Diringer, H. (1987) *J. Virol.* **61**, 3688–3693.
16. Kitamoto, T., Ogomori, K., Tateishi, J. & Prusiner, S. B. (1987) *Lab. Invest.* **57**, 230–236.
17. Serban, D., Taraboulos, A., DeArmond, S. J. & Prusiner, S. B. (1990) *Neurology* **40**, 110–117.
18. Taraboulos, A., Serban, D. & Prusiner, S. B. (1990) *J. Cell Biol.* **110**, 2117–2132.
19. DeArmond, S. J., McKinley, M. P., Barry, R. A., Braunfeld, M. B., McColloch, J. R. & Prusiner, S. B. (1985) *Cell* **41**, 221–235.
20. Cassab, G. I. & Varner, J. E. (1987) *J. Cell Biol.* **105**, 2581–2588.
21. Reisinger, P. W. M. & Unger, J. W. (1990) *Electrophoresis* **11**, 531–534.
22. Pont-Lezica, R. F. & Varner, J. E. (1989) *Anal. Biochem.* **182**, 336–337.
23. Barry, R. A., Vincent, M. T., Kent, S. B. H., Hood, L. E. & Prusiner, S. B. (1988) *J. Immunol.* **140**, 1188–1193.
24. Lowenstein, D. H., Butler, D. A., Westaway, D., McKinley, M. P., DeArmond, S. J. & Prusiner, S. B. (1990) *Mol. Cell. Biol.* **10**, 1153–1163.
25. Rogers, M., Serban, D., Gyuris, T., Scott, M., Torchia, T. & Prusiner, S. B. (1991) *J. Immunol.* **147**, 3568–3574.
26. Barry, R. A. & Prusiner, S. B. (1986) *J. Infect. Dis.* **154**, 518–521.
27. Laemmli, U. K. (1970) *Nature (London)* **227**, 680–685.
28. Prusiner, S. B., Bolton, D. C., Groth, D. F., Bowman, K. A., Cochran, S. P. & McKinley, M. P. (1982) *Biochemistry* **21**, 6942–6950.
29. Marsh, R. F. & Kimberlin, R. H. (1975) *J. Infect. Dis.* **131**, 104–110.
30. Liberski, P. P., Yanagihara, R., Gibbs, C. J. J. & Gajdusek, D. C. (1989) *Acta Neuropathol.* **79**, 1–9.
31. Kimberlin, R. H., Field, H. J. & Walker, C. A. (1983) *J. Gen. Virol.* **64**, 713–716.
32. Fraser, H. & Dickinson, A. G. (1985) *Brain Res.* **346**, 32–41.
33. Stahl, N., Borchelt, D. R., Hsiao, K. & Prusiner, S. B. (1987) *Cell* **51**, 229–240.
34. McKinley, M. P., Taraboulos, A., Kenaga, L., Serban, D., Stieber, A., DeArmond, S. J., Prusiner, S. B. & Gonatas, N. (1991) *Lab. Invest.* **65**, 622–630.
35. Bockman, J. M., Kingsbury, D. T., McKinley, M. P., Bendheim, P. E. & Prusiner, S. B. (1985) *N. Engl. J. Med.* **312**, 73–78.
36. Wisniewski, H. M., Bancher, C., Barcikowska, M., Wen, G. Y. & Currie, J. (1989) *Acta Neuropathol.* **78**, 337–347.
37. Kretzschmar, H. A., Prusiner, S. B., Stowring, L. E. & DeArmond, S. J. (1986) *Am. J. Pathol.* **122**, 1–5.
38. Hecker, R., Taraboulos, A., Scott, M., Pan, K.-M., Torchia, M., Jendroska, K., DeArmond, S. J. & Prusiner, S. B. (1992) *Genes Dev.* **6**, 1213–1228.
39. McGrath, C. M., Grudzien, J. L., Decker, D. A. & Robbins, T. O. (1991) *BioTechniques* **11**, 352–361.